forests

MDPI

Article

Design of Vibration and Noise Reduction for Ultra-Thin Cemented Carbide Circular Saw Blades in Woodworking Based on Multi-Objective Optimization

Na Jia, Lei Guo, Ruisen Wang and Jiuqing Liu *

College of Mechanical and Electrical Engineering, Northeast Forestry University, Harbin 150040, China; jiana@nefu.edu.cn (N.J.); gl1999@nefu.edu.cn (L.G.); 15144684021@nefu.edu.cn (R.W.)
* Correspondence: nefujdljq@163.com

Abstract: Cemented carbide circular saw blades are widely used for wood cutting, but they often suffer from vibration and noise issues. This study presents a multi-objective optimization method that integrates ANSYS and MATLAB to optimize the design of noise reduction slots in circular saw blades. A mathematical model was developed to correlate the emitted sound power with the overall vibration intensity. A multi-objective optimization model was then formulated to map the slot shape parameters to the deformation, equivalent stress, and vibration intensity during sawing. The ABAQUS thermal–mechanical coupling analysis was used to determine the sawing force and temperature field. The NSGA-II algorithm was applied on the ANSYS–MATLAB platform to iteratively compute slot shape parameters and conduct optimization searches for a globally optimal solution. Circular saw blades were fabricated based on the optimization results, and experimental results showed a significant reduction in sawing noise by 2.4 dB to 3.0 dB on average. The noise reduction effect within the specified frequency range closely agreed with the simulation results, validating the method's efficiency. This study provides a feasible and cost-effective solution to the multi-objective optimization design problem of noise reduction slots for circular saw blades.

Keywords: circular saw blade; vibration and noise reduction; multi-objective optimization; co-simulation; noise reduction slot

Citation: Jia, N.; Guo, L.; Wang, R.; Liu, J. Design of Vibration and Noise Reduction for Ultra-Thin Cemented Carbide Circular Saw Blades in Woodworking Based on Multi-Objective Optimization. *Forests* **2024**, *15*, 1554. https://doi.org/10.3390/f15091554

Academic Editors: Ján Kováč, Richard Kminiak and Paweł Tylek

Received: 27 July 2024
Revised: 15 August 2024
Accepted: 2 September 2024
Published: 3 September 2024

1. Introduction

Cemented carbide circular saw blades demonstrate extremely high processing efficiency and service life in wood cutting processes due to their outstanding hardness and wear resistance. However, as the demand for processing precision and resource efficiency increases, traditional thick cemented carbide circular saw blades show limitations in handling expensive or delicate materials. This has prompted a shift in the study focus of circular saw blade technology towards ultra-thin cemented carbide circular saw blades. By decreasing the thickness of the saw blade, material waste, energy usage and heat production while cutting can be dramatically reduced, thereby improving cutting efficiency and processing quality.

However, due to its high aspect ratio, this type of circular saw blade typically exhibits lower lateral rigidity, which can lead to pronounced vibration and extensive noise [1]. Vibration and noise not only affect operator comfort and safety, but also have a negative impact on the working life of the saw blade and sawing quality. The tooling industry's growing emphasis on environmental and green manufacture has made the control of vibration and noise a crucial technical obstacle in the production of ultra-thin carbide circular saw blades. The development of effective vibration and noise suppression technologies is not only a necessary way to improve the performance of circular saw blades but also an important strategy to drive the industry towards sustainable development.

The circular saw blade is the main source of both noise and vibration in the sawing mechanism. Hence, the noise generated during the operation of sawing can be significantly diminished by implementing a well-planned optimization design for the construction of the circular saw blade. M. S. Bobeczko discovered that creating grooves in a precise location on a small saw blade could greatly reduce the noise produced when cutting aluminum sheets [2]. Several scholars have since examined how the shape, position, length, and quantity of saw blade slot holes affect the degree of vibration noise produced by circular saw blades [3–7]. A study has proved that the presence of slotted hole structures in circular saw blades efficiently impedes vibrations by reducing the speed at which vibration waves travel, consequently interrupting the mechanism that generates noise. In addition, several experts have suggested slot hole designs for circular saw blades. Chen et al. and Gau et al. used the largest difference between the natural frequency and the rotational frequency of the circular saw blade as a criterion for optimizing the sizes of slots [8,9]. Wu et al. employed a variable density topology optimization method to detect areas of low pseudo-density on the substrate of the saw blade in order to optimize the placement of slot holes [10]. Furthermore, Tian et al. developed a low-noise slotted circular saw blade using a sequential response surface optimization method [11].

Although there has been significant development in previous studies about the optimization of slot size and positional characteristics of circular saw blades, the overall design of the slots has remained relatively unexplored. Currently, there is no established theoretical framework that explicitly links the shape parameters of the slot hole structure to the vibration noise performance of the circular saw blade during operation. This lack of correlation hinders the scientific and practical aspects of designing ideal slots for circular saw blades. In addition, as the circular saw blade substrate becomes thinner, the decrease in its lateral stiffness makes it difficult to ensure the overall safety of the structure through a single objective strategy.

Multi-objective optimization is essential in this setting. This method effectively achieves a balance between controlling vibration noise and ensuring structural safety. It optimizes the size, shape, and layout of the slot hole while also maintaining its security. NSGA-II is a multi-objective optimization algorithm that utilizes the genetic algorithm framework and incorporates elite strategies [12]. The coding mechanism of this algorithm is highly adaptable, and it is widely used in the optimization of energy system operations [13], machining process parameters [14], material distribution [15], production scheduling [16], and structural dimension optimization [17]. Its flexible coding features make it an ideal choice for handling the optimization models of saw blade shape parameters.

This study employs a multi-objective optimization technique to address the issue of noise reduction slot design for ultra-thin cemented carbide circular saw blades utilized as particleboard saws. A combination of mathematical modeling, experimental design, thermal–mechanical coupling simulation, topology optimization, and co-simulation techniques is used to establish the relationship between the shape parameters of circular saw blade slot holes and sawing quality, safety, and vibration noise performance. A co-simulation platform, which operates in real time, has been constructed using ANSYS 2021 R1 and MATLAB R2021a. ANSYS is used on this platform to perform the parametric modeling of saw blades and conduct simulation calculations for sawing deformation, equivalent stress, and vibration response. NSGA-II is called by MATLAB to repeatedly optimize the parameters of the saw blade slot shape and find the best solution that meets the comprehensive performance index. The actual application of the proposed multi-objective optimization method is confirmed by sawing experiments of particleboard, demonstrating its feasibility and effectiveness.

2. Mathematical Model

The most straightforward optimization approach to achieve the vibration and noise reduction of circular saw blades is to consider the sawing noise as the goal function and aim to minimize it. Nevertheless, the computing demands of the acoustic coupling model

in the sawing system are high, and the optimization calculation procedure, which involves a large number of iterations, incurs a substantial cost that is challenging to align with the practical engineering needs. Hence, it is imperative to develop alternative strategies for noise forecasting and to incorporate the utilization of effective optimization techniques.

2.1. Circular Saw Blade Vibration and Noise Calculation Model

Equation (1) illustrates how vibration and noise in the circular saw blade sawing process are related to each other. This formula is known as the surface radiation noise power formula [18]:

$$W = \rho_0 c \sigma_{rad} A < \bar{v^2} > \tag{1}$$

where W represents the radiation sound power, $\rho_0 c$ represents the characteristic impedance, σ_{rad} represents the acoustic radiation coefficient, A represents the effective radiation area, and $\bar{v^2}$ represents the Root-Mean-Square (RMS) surface velocity of the circular saw blade. If the material, size, and working speed of the circular saw blade are already established, the RMS surface velocity of the circular saw blade is directly proportional to the noise power emitted. Hence, the crucial factor in reducing the noise radiation energy and enhancing rotational stability is to suppress the RMS surface velocity of the circular saw blade. This study presents a method for mathematically calculating the RMS surface velocity of the circular saw blade. The goal of this method is to reduce computational complexity and volume and to quickly assess the impact of the slot-hole vibration and noise reduction for efficient design iteration and optimization. By applying the fundamental principles of Kirchhoff's thin-plate theory, the complex three-dimensional stress analysis of a circular saw blade sawing is reduced to a simpler two-dimensional plane stress analysis. Furthermore, the calculation of the circular saw blade's vibration displacement can be achieved by converting the vibration equation of the blade into a linear combination of vibrations from several undamped single-degree-of-freedom systems [19]. This transformation allows us to describe the vibration equation as Equation (2):

$$z(x,t) = \sum_{n=1}^{N} \phi_n(x) q_n(t) \tag{2}$$

where $z(x,t)$ represents the transverse displacement of a circular saw blade at a specific position x and time t, N represents the modal truncation order, $\phi_n(x)$ represents the mode shape function of the nth mode, and $q_n(t)$ represents the generalized coordinate of the nth mode, which is expressed as Equation (3):

$$q_n(t) = X_n \cos(\omega_n t + \varphi_n) \tag{3}$$

where X_n represents the vibration amplitude of the nth mode, ω_n represents the natural frequency of the nth mode, and ϕ_n represents the initial phase of the nth mode. The RMS surface velocity of the circular saw blade in various vibration periods Tn is derived and computed using Equations (4)–(7):

$$v(x,t) = \frac{\partial z(x,t)}{\partial t} = -\sum_{n=1}^{N} Xn\omega_n \phi_n(x) \sin(\omega_n t + \varphi_n) \tag{4}$$

$$v^2(x,t) = \sum_{n=1}^{N} Xn^2 \omega_n^2 \phi_n(x)^2 \sin^2(\omega_n t + \varphi_n) \tag{5}$$

$$< \bar{v^2} > = \sum_{n=1}^{N} \frac{1}{2Tn} \int_0^{Tn} Xn^2 \omega_n^2 \phi_n(x)^2 [1 - \cos 2(\omega_n t + \varphi_n)] \mathrm{d}t \tag{6}$$

$$< \bar{v^2} > = \frac{1}{2} \sum_{n=1}^{N} Xn^2 \omega_n^2 \phi_n(x)^2 \tag{7}$$

As shown in Figure 1, the vibration modes of circular saw blades are primarily determined by their structural properties, specifically, the number of nodal diameters and the number of nodal circles. When the circular saw blade vibrates, it generates several sinusoidal waveforms [20]. Thus, to precisely evaluate the impact of various regions on vibration noise in different vibration patterns of the circular saw blade and subsequently conduct vibration and noise reduction design, it is essential to divide the circular saw blade surface into multiple elements. The formula for calculating the radiation sound power W can then be represented by Equation (8):

$$W = \frac{1}{2}\rho_0 c \sum_i \sigma_i A_i \sum_{n=1}^{N} Xn^2 \phi_{n,i}^2(x)\omega_n^2 \tag{8}$$

where σ_i represents the sound radiation coefficient of the ith element, A_i represents the effective radiation area of the ith element, and $\phi_{n,i}(x)$ represents the shape function of the nth order mode on the ith element. According to the aforementioned analysis, it is observed that the noise radiation intensity of a circular saw blade is determined by the product of the area A_i of each unit of the blade and the vibration displacement u_i of that unit. The product is defined as the "overall vibration intensity S" [21], and its formula is provided in Equation (9):

$$S = \sum_i A_i u_i = \sum_i A_i \left| \sum_{n=1}^{N} \phi_{n,i} X_n \right| \tag{9}$$

Controlling the overall vibration intensity of circular saw blades is a viable method for diminishing noise emission from sawing devices. Therefore, the issue can be expressed mathematically as an optimization problem with the objective of minimizing the overall vibration intensity. During the optimization process, calculations are performed to determine the vibration response of the circular saw blade at each frequency. The overall vibration intensity is then assessed, resulting in a substantial reduction in the complexity of calculations required.

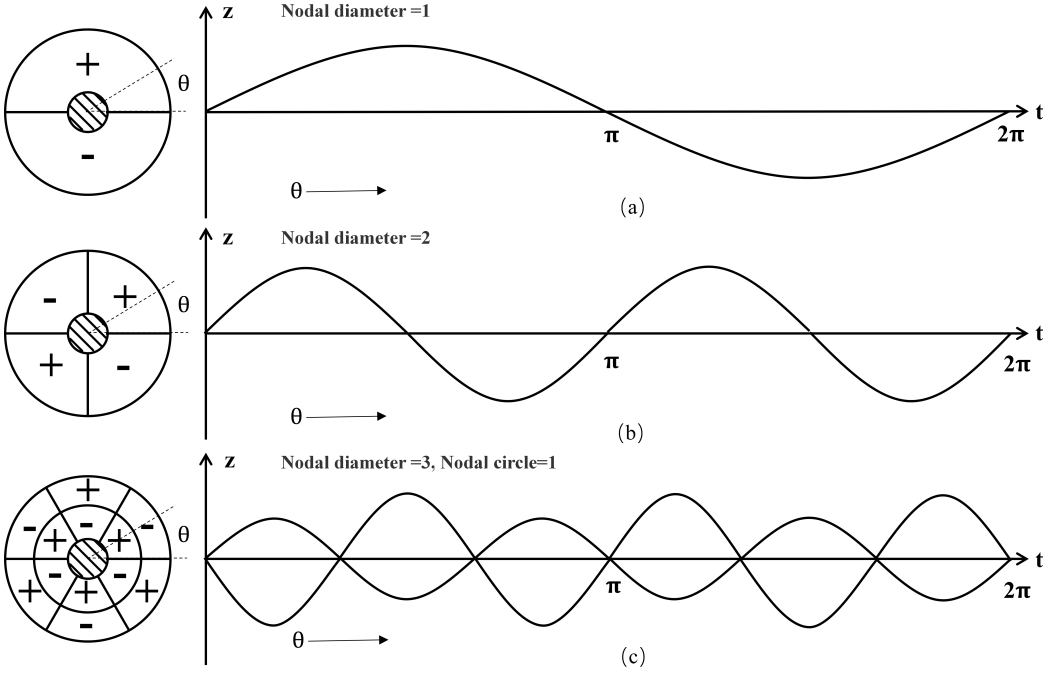

Figure 1. Circular saw blade's different vibration patterns.

2.2. Multi-Objective Optimization Model

In this study, an ultra-thin cemented carbide circular saw blade was selected, and its specific dimensional parameters can be found in Table 1. To address the optimization issue of the noise reduction slot, a parametric modeling approach was used. This method established a direct mapping relationship between the shape parameters and the finite element calculation results. By taking into account multiple design objectives that were mutually constrained, an optimization scheme was derived.

Table 1. Parameters of circular saw blade.

Diameter (mm)	Aperture (mm)	Tooth Number (T)	Tooth Width (mm)	Saw Blade Thickness (mm)	Flange Diameter (mm)	Serration Type
305	30	100	2	1.5	120	Trapezoidal serrated

1. Optimization objective.
The optimization targets for ensuring machining quality, safety, and reducing vibration and noise following grooving are the maximum deformation (y_1), the maximum equivalent stress (y_2), and the cumulative sum of overall vibration intensity (y_3). The maximum deformation represents the deflection deformation capacity of the circular saw blade during the cutting process. Excessive deformation can result in interference between the circular saw blade and the workpiece, affecting machining accuracy and surface quality. By regulating the level of deformation within an acceptable range, one may guarantee that the circular saw blades maintain high processing quality following grooving [22]. The maximum equivalent stress shows the general stress level experienced by the circular saw blade when subjected to a cutting load. Excessive equivalent stress can result in plastic deformation, cracking, and other failures of the circular saw blade, compromising its safety during use. Optimizing the maximum equivalent stress can increase the strength and service life of circular saw blades [23]. The cumulative sum of the overall vibration intensity (y_3) represents the total sum of the vibration intensity of the circular saw blade when subjected to various excitations. This target value effectively captures the vibration noise characteristics of the slotted circular saw blade across a wide range of frequencies.
2. Design domain.
The Variable Density Topology Optimization approach, based on the Solid Isotropic Material with Penalization (SIMP) technique, was employed to manipulate the cell pseudo-density of a finite element model of a circular saw blade. The objective was to achieve convergence to either 0 or 1 by incorporating a penalty factor. A pseudo-density close to 1 indicates material retention, while a value close to 0 signifies material removal. This method determines the design domain of the noise reduction slot on the circular saw blade [24].
The topology optimization zone of the circular saw blade was defined as a substrate by removing the serrated and the flange clamping section. The goal of the optimization was to maximize the structural rigidity of the circular saw blade. During the optimization phase, the circular saw blade design was considered for its symmetry to provide evenness and stability during loading and utilization. The improved circular saw blade model underwent a surface trimming procedure, and the design domain for the slot holes was chosen to be the low-density zone with a significant area, as depicted in Figure 2.

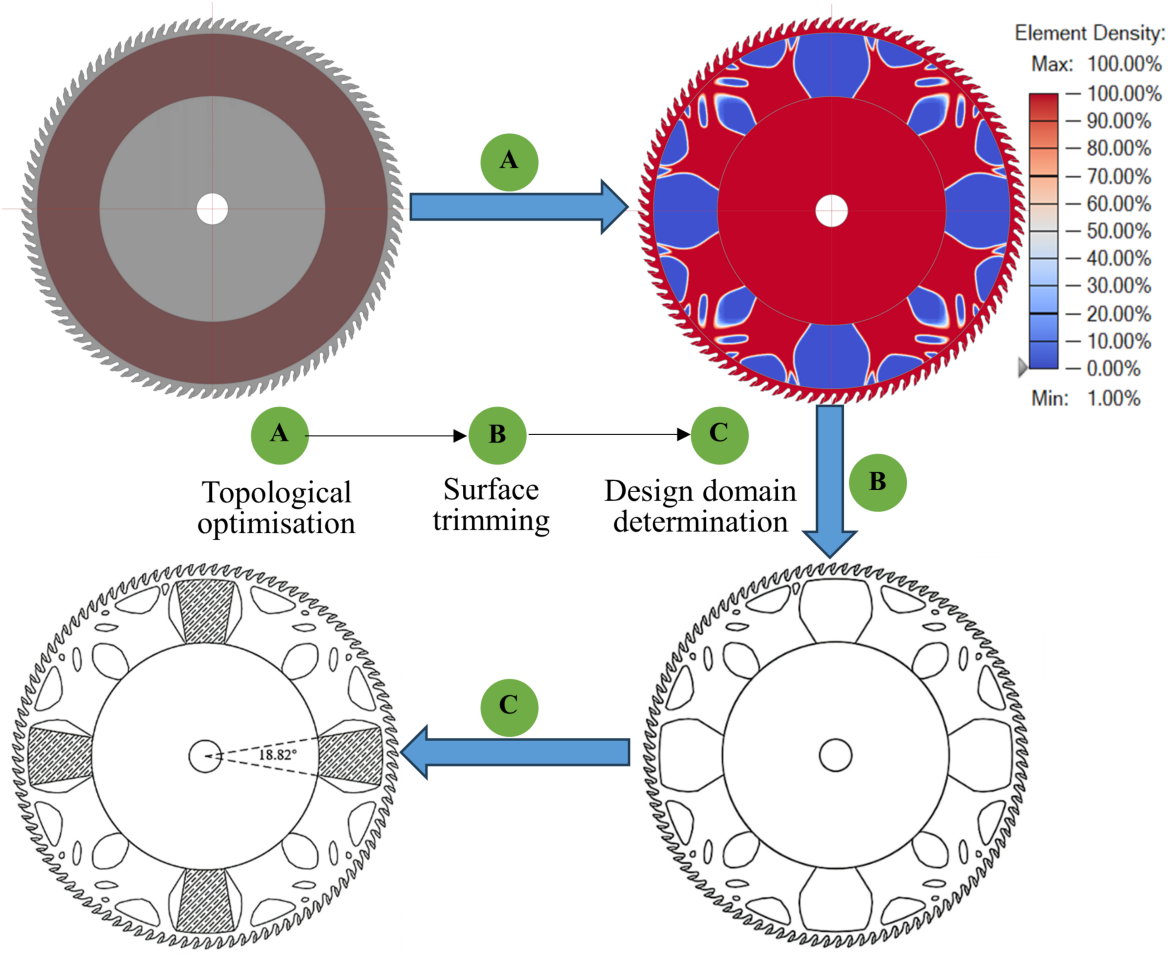

Figure 2. Determination process for the design domain of noise reduction slots.

3. Design variables and parametric modeling.

Due to the distribution of the low-density region along the radial direction of the circular saw blade, a radial slot was selected for opening. The circular saw blade's shape parameters encompassed the slot's position and size. The exact stages and outcomes of the parametric modeling approach are illustrated in Figure 3. Initially, the geometric characteristics of the key spots in the slot holes of the circular saw blade substrate were determined. This included identifying the starting point, finishing point, and the positioning information of the four equidistant intermediate locations. An interpolation technique was used to achieve the positional value addition and translation of the information points. The whole contour of the slot was formed by connecting these essential locations with a smooth curve. Subsequently, stress relief holes were strategically constructed and created at the two terminal positions of the slot in order to minimize stress concentration and improve the overall structural integrity [25]. The circular saw blade model was modified by incorporating a sound deadening slot with stress relief holes, resulting in the final circular saw blade model that included the noise reduction slot.

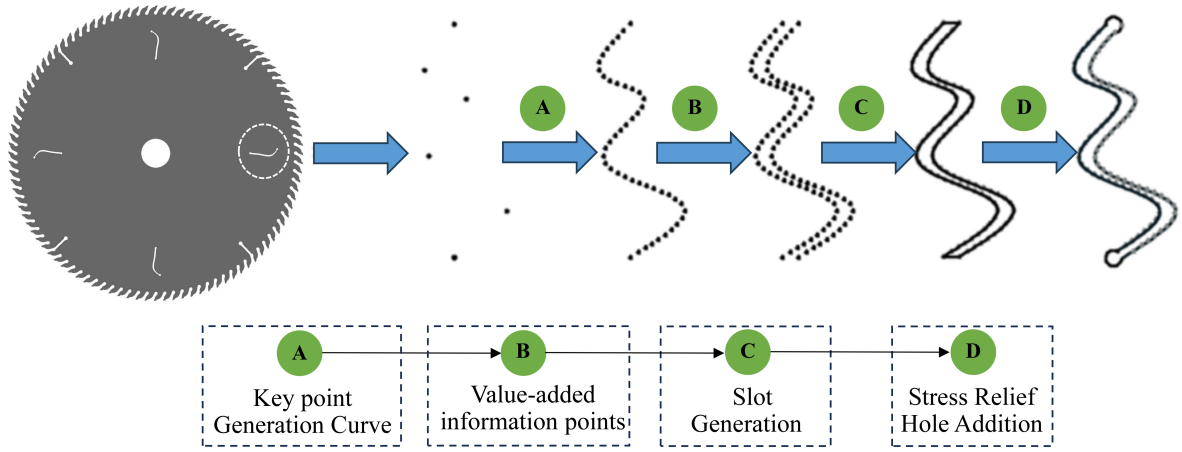

Figure 3. Parametric modeling of circular saw blade with noise reduction slot.

This study developed nine important design factors to precisely characterize the geometric information of the critical spots, which were the initial radius x_1, the final radius x_2, the width of the slot x_3, the starting point, the ending point, and the angles of the four equidistant intermediate key points x_4 to x_9. The variables were consolidated into a shape parameter vector (Equation (10)), which acted as the independent variable in the optimization model:

$$x^T = \{x_1, x_2, x_3, x_4, x_5, x_6, x_7, x_8, x_9\}^T \tag{10}$$

Table 2 displays the range of values for the constrained design variables. This was to ensure that the matrix slot holes were created within a specific design region and to prevent any negative impact on the mesh quality near the holes due to flanges or other restrictions.

Table 2. Design variables and range of values.

Design Variable	Variable Description	Minimum Value	Maximum Value
x_1	Starting radius	95 mm	105 mm
x_2	Terminal radius	125 mm	135 mm
x_3	Slot width	0.5 mm	1 mm
$x_4 \sim x_9$	Key point angle	−9.41°	9.41°

4. Multi-objective optimization model.

Utilizing the aforementioned principles, a mathematical model for multi-objective optimization was formulated to design noise-reducing slots in circular saw blades. The objective was to create circular saw blades that satisfied the criteria of stiffness and strength, while also possessing low noise properties. The aim was to minimize the optimization objective function $f(x)$ comprised of the maximum deformation, the maximum equivalent stress, and the cumulative sum of overall vibration intensity. Equation (11) defined the mathematical model:

$$\begin{aligned} &\min f(x) = f(y_1(x), y_2(x), y_3(x)) \\ &s.t. \begin{cases} 95\,\text{mm} < x_1 < 105\,\text{mm} \\ 125\,\text{mm} < x_2 < 135\,\text{mm} \\ 0.5\,\text{mm} < x_3 < 1\,\text{mm} \\ 0^\circ < x_4, x_5, x_6, x_7, x_8, x_9 < 18.82^\circ \end{cases} \end{aligned} \tag{11}$$

3. Optimization Case Study

3.1. Materials

Table 1 displays the dimensional characteristics of the circular saw blade utilized in this research, which included four thermal expansion slots. The body material of the circular saw blade was SKS51 and the serrated material was YG6. The parameters of these materials are shown in Table 3.

Particleboard is a kind of man-made board made from wood waste as raw material, mechanically shredded, dried and heated to form. It has good mechanical properties, dimensional stability, and processing performance. Due of its prevalence in the furniture and building decoration industry, it was selected as the subject of study for sawing purposes.

Precisely determining the characteristics of the material being cut is essential for designing an effective noise reduction slot. However, particleboard, due to its distinct structure and composition, has physical and mechanical properties that differ significantly from traditional wood or other engineering materials. Material parameters obtained from experience or the literature often do not meet the requirements for highly accurate simulation, as they may not adequately describe a specific batch or type of particleboard material. Therefore, this study investigated the physical and mechanical properties of particleboard through experimental testing.

Although particleboard is anisotropic, the fiber orientation of the material is substantially weakened by the mixing of the particles with the glue layer, which is isotropic and homogeneous throughout the plane. However, material properties are different at different thickness levels [26]. To streamline the constitutive model, the simulation procedure disregarded the impact of unequal proportions of shavings and glue layers during particleboard manufacture. Consequently, the particleboard was treated as an isotropic material.

In accordance with the standard GB/T 17657-2022 "Test Methods for Physical and Chemical Properties of Wood-based Panels and Decorative Wood-based Panels" [27], the constitutive parameters of particleboard were calibrated on a WDW-300E testing machine. The thermodynamic performance parameters were referred to in [28]. The experimental process is illustrated in Figure 4, and the results are presented in Table 4.

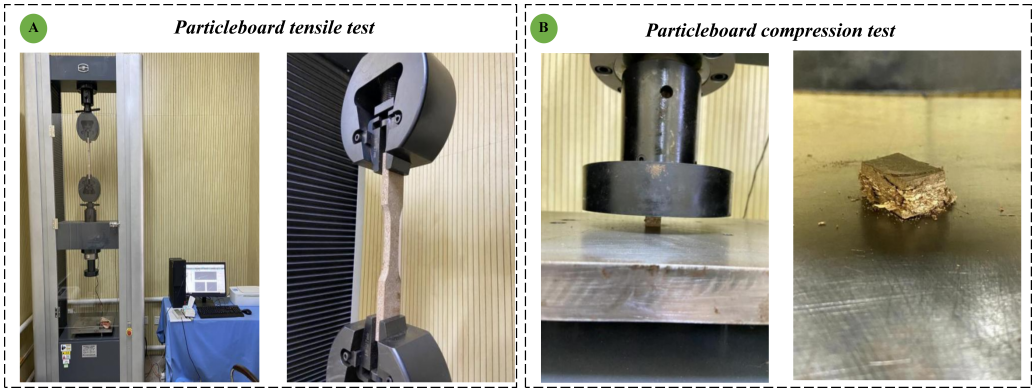

Figure 4. Test of physical and mechanical properties of particleboard.

Table 3. Saw body and serrated material properties.

Materials	SKS51 (Saw Body)	YG6 (Serrated)
Density (kg/m^3)	7850	14,800
Poisson's ratio	0.28	0.30
Modulus of elasticity (GPa)	210	510
Coefficient of thermal expansion (1/K)	11.2×10^{-6}	6×10^{-6}
Specific heat (J/kg°C)	460	220
Thermal conductivity (W/mK)	51.9	75.0

Table 4. Physical and mechanical properties of test particleboards.

Property	Density (g/cm^3)	Poisson's Ratio	Modulus of Elasticity (MPa)	Bending Strength (MPa)	Coefficient of Thermal Expansion (1/K)	Specific Heat (J/kg°C)	Thermal Conductivity (W/mK)
Particleboard	0.65	0.342	5204	79	6.9×10^{-6}	1900	0.165

3.2. Analysis of Simulation Models

To accurately calculate the maximum deformation, equivalent stress, and overall vibration intensity of the circular saw blade during the sawing process, a sawing thermal–mechanical coupling model was established first. This model obtained the prestressed state of the circular saw blade under the action of the sawing load and temperature field by simulating the load conditions and temperature field during the sawing process. This state was a key basis for calculating the maximum deformation, equivalent stress, and natural frequency of the circular saw blade and further evaluating its sawing performance and safety. Based on the obtained stress state, the natural frequency of the saw blade was further calculated by using the prestressed modal analysis method. On this basis, excitation forces of multiple frequencies were applied to the circular saw blade to calculate its overall vibration intensity in a wide frequency band. The simulation process is shown in Figure 5.

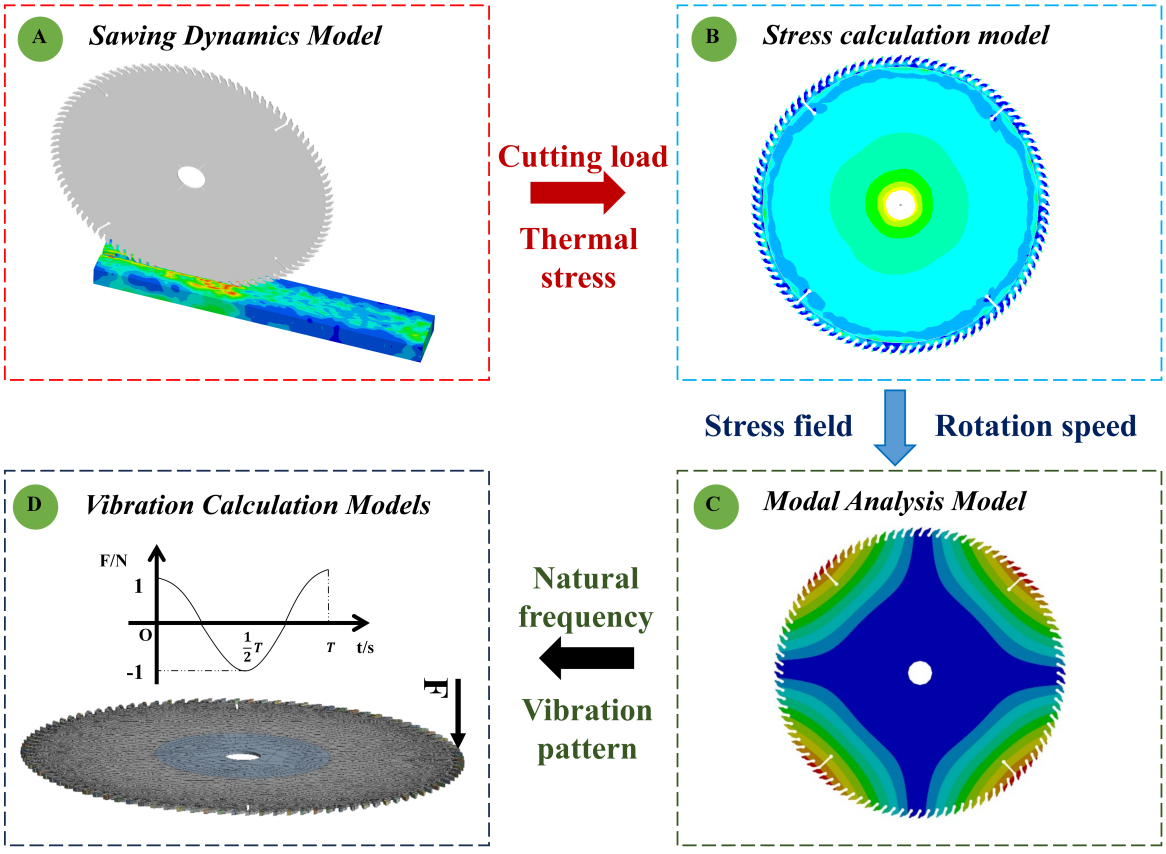

Figure 5. Simulation process.

3.2.1. Thermal–Mechanical Coupling Sawing Model Analysis

The sawing process is an intense thermal–mechanical coupling process. This study employed the ABAQUS dynamics/explicit module to create a simulation model for the thermal–mechanical coupling. The circular saw blade and flange constituted a rotating structure, and with the addition of particleboard, an intact sawing model was established,

as illustrated in Figure 6. The boundary conditions were defined as follows: the circular saw blade rotated at a speed of 3000 r/min, with a relative feed rate of 4 m/min and a cutting depth of 2 mm.

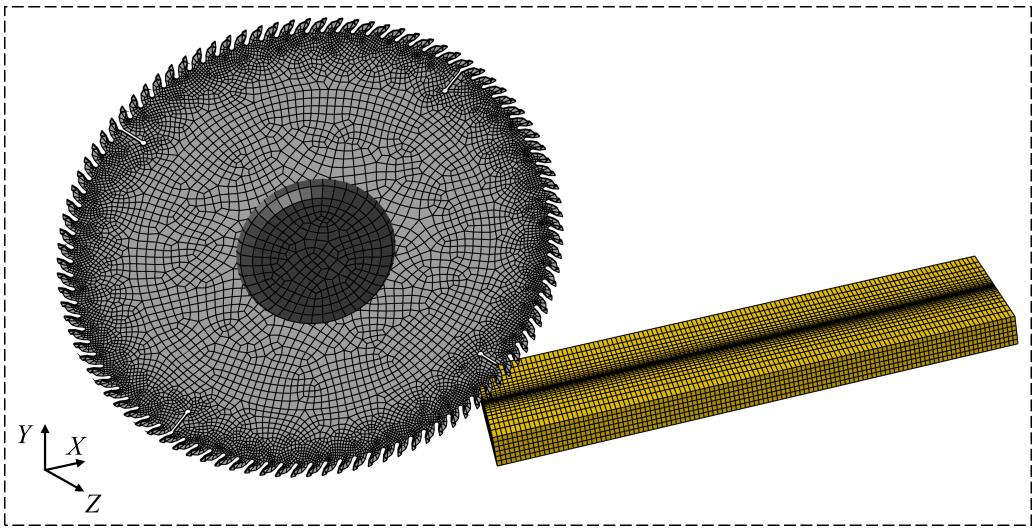

Figure 6. Thermal–mechanical coupling calculation model for the saw cutting system.

The dynamic contact between the circular saw blade and the particleboard was modeled as sliding friction following Coulomb's law. This contact relationship was handled using a penalty function-based node-to-surface contact algorithm. The dynamic and static friction coefficients between the saw teeth, saw body, and particleboard were set to 0.35 and 0.4, respectively [29]. In addition, it was assumed that about 60% of the frictional energy generated by the saw blade and chips during sawing was converted into thermal energy [30,31], and therefore, this thermal energy conversion ratio was set to 0.6.

Given the large surface area of the circular saw blade, forced convection induced by rotation leads to a cooling effect on the blade. In addition to convective heat transfer over the laminar and turbulent surface regions, the saw teeth and thermal expansion slots also contribute to heat dissipation. Based on the empirical formulas summarized in references for calculating the convective heat transfer coefficients in different regions of a circular saw blade [32,33], the following values were assigned: the convective heat transfer coefficient in the laminar region was set to 40.47 W/mK), the coefficient in the turbulent region was set to 79.60 W/mK), and the coefficient at the blade edge was set to 2120.46 W/mK).

When thermal–mechanical coupling simulation was carried out in ABAQUS 2023, the support reaction force included not only the reaction force of the cut workpiece on the tool but also the additional reaction force due to the thermal expansion effect. In this study, the support and reaction force of the rotary saw blade were coupled to a node at the inner hole of the saw blade in order to obtain the magnitude of the cutting force and the rule of change. The sawing duration was set to 5 s, and the calculation interval step was 0.025 s. The calculation results of the cutting force of the circular saw blade for each statistical step length are shown in Figure 7. The temperature change of the circular saw blade is shown in Figure 8. The initial temperature of the circular saw blade is depicted in Figure 8a, while Figure 8b shows the temperature distribution at t = 4.75 s.

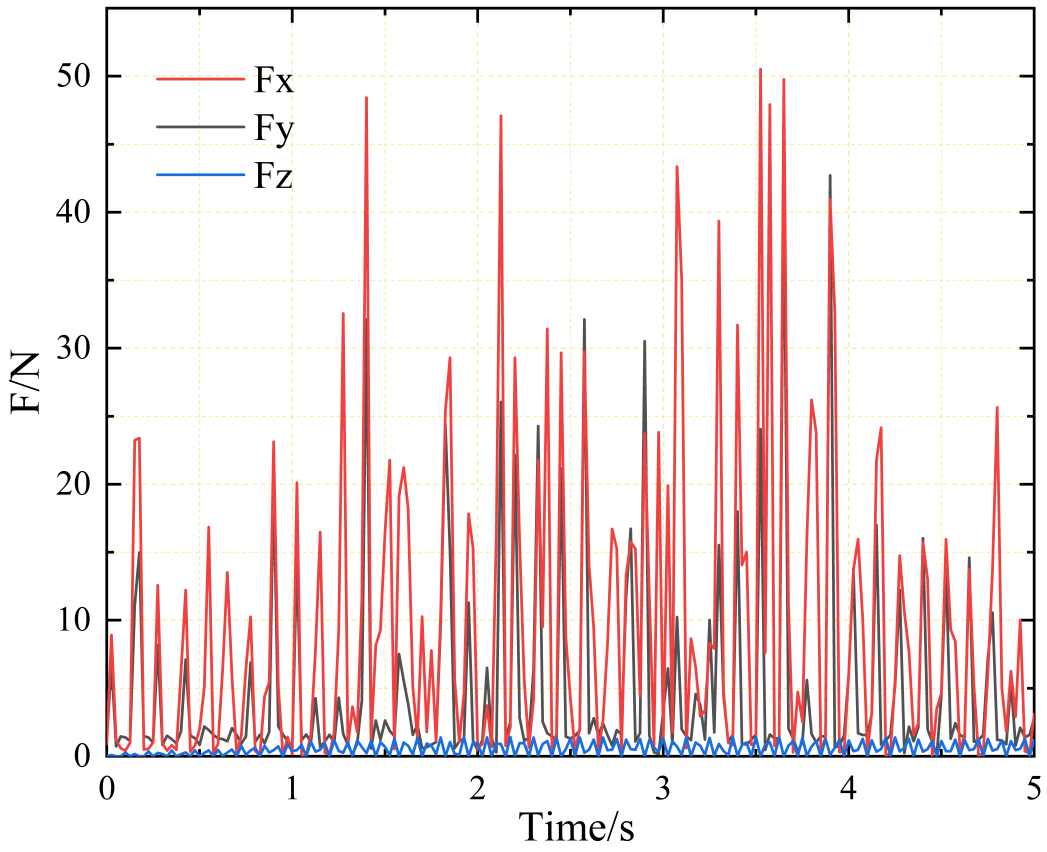

Figure 7. Cutting force of circular saw blade in X, Y, and Z directions.

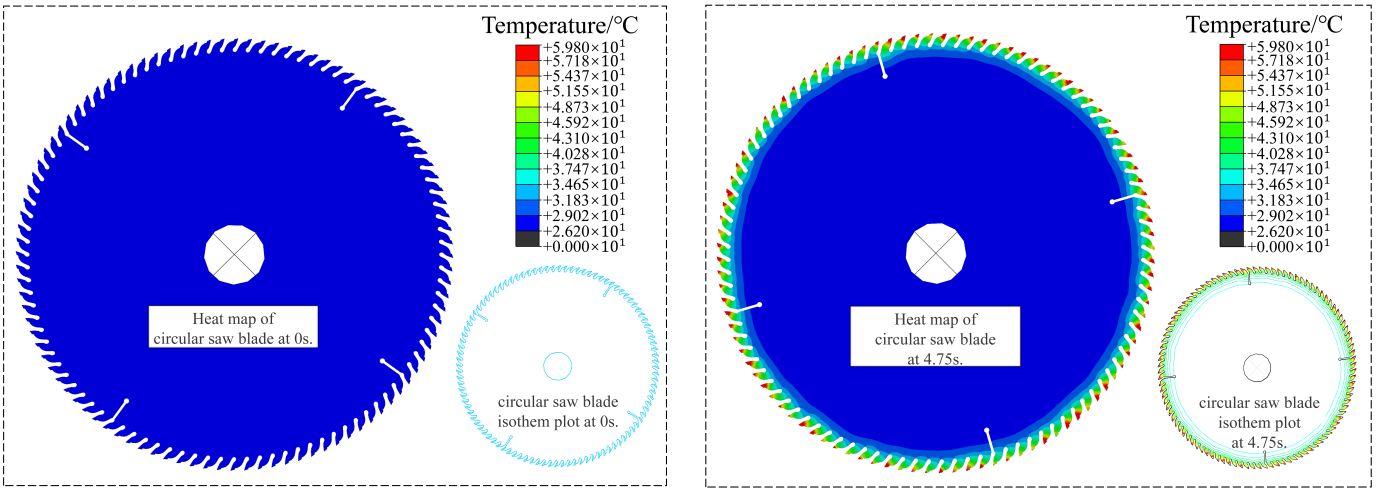

(**a**) Time t = 0 s, temperature = 26.2 °C (**b**) Time t = 4.75 s, temperature = 59.8 °C

Figure 8. Temperature and isotherm variation curve of circular saw blade.

3.2.2. Calculation Model for Stress and Natural Frequency of Circular Saw Blades

After determining the sawing load and temperature distribution of the circular saw blade, this study utilized the ANSYS APDL static module to create a stress simulation model for calculating the stress state and natural frequency of the circular saw blade. Yu et al. [34] found that the circular saw blade experienced increased natural frequency as a result of the stiff action caused by centrifugal tensile tension during rotation. Nevertheless, the strain resulting from the thermal effects of cutting decreases the natural frequency of the circular saw blade. While the tangential compressive stress resulting from heat expansion is minor, the primary factor contributing to the outward expansion of the circular saw blade

is the tensile stress. Additionally, the impact of cutting stress on the natural frequency is minimal. To precisely mimic the initial stress state and deformation characteristics of ultra-thin circular saw blades, we chose to use the Shell 181 shell element to develop the model of the circular saw blade. In this model, all constraints were imposed on the inner hole of the saw blade, while all constraints were imposed on the flange region except for axial rotation. Subsequently, the circular saw blade experienced centrifugal stress according to its rotational speed. The sawing load and temperature field, derived by thermodynamic coupling simulation, were then fed into the saw blade model to calculate the stress field. The maximum deformation, equivalent stress, and natural frequency of a circular saw blade under prestress were estimated using the approach of linear perturbation analysis. The calculation results displayed the initial 50 natural frequencies and some modal vibration patterns, as depicted in Figure 9.

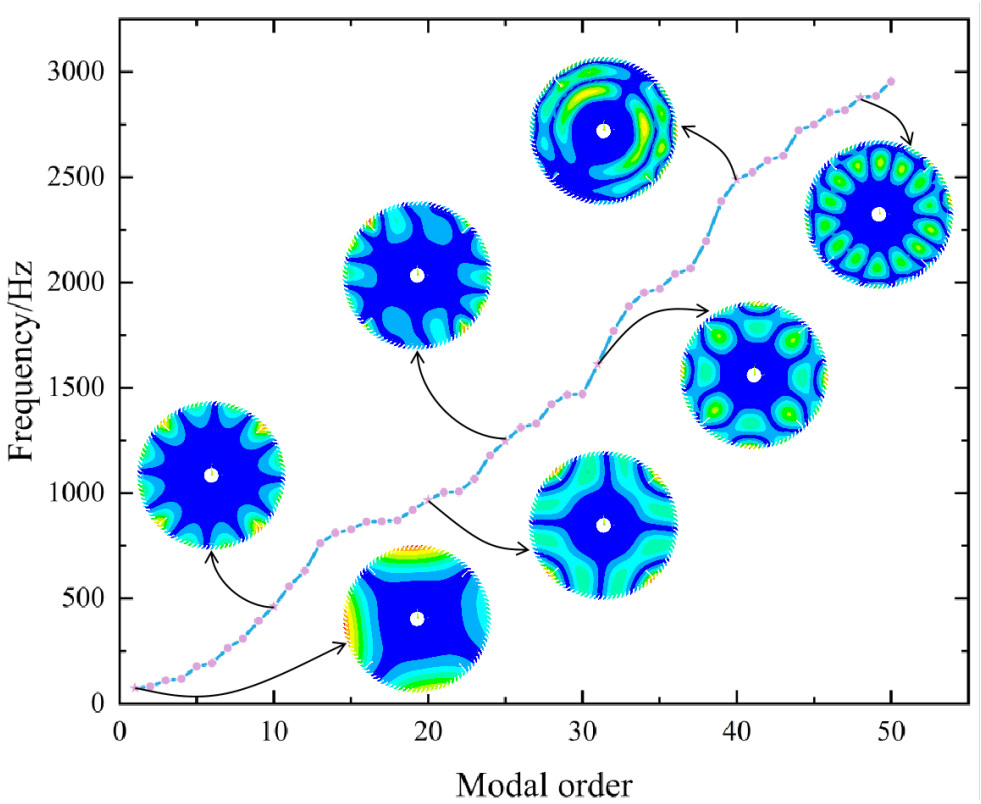

Figure 9. The inherent frequencies and some modal vibration patterns of the first 50 modes of the circular saw blade.

3.2.3. Calculation Model for Overall Vibration Intensity of Circular Saw Blades

Upon analyzing Figure 9, it is evident that the natural frequency distribution of the circular saw blade is very concentrated. The anisotropic mechanical properties of particleboard, coupled with the predominantly manual feeding approach adopted by most panel saws, lead to fluctuations in the lateral excitation frequency during the cutting process [35]. These factors make it difficult to completely avoid all potential resonance frequencies through the use of noise reduction slots. Hence, it is imperative to implement a strategy that aims to decrease the magnitude of vibrations and optimize vibration distribution in order to minimize the emission of noise during the process of sawing [36]. The ANSYS APDL harmonic response analysis module was utilized to compute the vibration response of a circular saw blade across a large frequency range. The mode superposition method was employed to determine the actual displacement of each node under various stimulation frequencies. By converting the vibration equation from the space coordinate system to the modal coordinate system, and simplifying the complex multi-degree-of-freedom system to

the combination of several single-degree-of-freedom systems [37], the simplified vibration equation shown in Equation (12) was established:

$$(\boldsymbol{K} - \omega^2 \boldsymbol{M} + i\omega \boldsymbol{C})\{u\} = \{F_0\} \tag{12}$$

where $\boldsymbol{K}$, $\boldsymbol{M}$, and $\boldsymbol{C}$ represent the stiffness matrix, mass matrix, and damping matrix, respectively, $\{u\}$ represents the complex amplitude response of the structure under the load frequency ω, and $\{F_0\}$ represents the load amplitude matrix. The analytical frequency segment chosen for this study was 0 Hz to 2000 Hz. Lateral loads of 1 N were applied to the serrated nodes at intervals of 10 Hz. According to Equation (9), an array was defined to record the product of the response amplitudes of all nodes and their corresponding areas in each frequency step. By summing the results of each step length, the sum of the overall amplitude intensity was obtained.

3.3. ANSYS–MATLAB Collaborative Multi-Objective Optimization Method Based on NSGA-II

3.3.1. NSGA-II Multi-Objective Optimization Algorithm

This study utilized NSGA-II to acquire a set of Pareto optimal solutions for our multi-objective optimization problems. NSGA-II was introduced by Deb et al. as an enhancement to NSGA [38]. It incorporated a rapid non-dominated sorting approach and an elite retention strategy to prevent the loss of high-quality populations during the evolution process. Furthermore, the method incorporated the crowding comparison operator to augment population diversity, hence facilitating the search for global optima. Figure 10 illustrates the fundamental sequence of calculations.

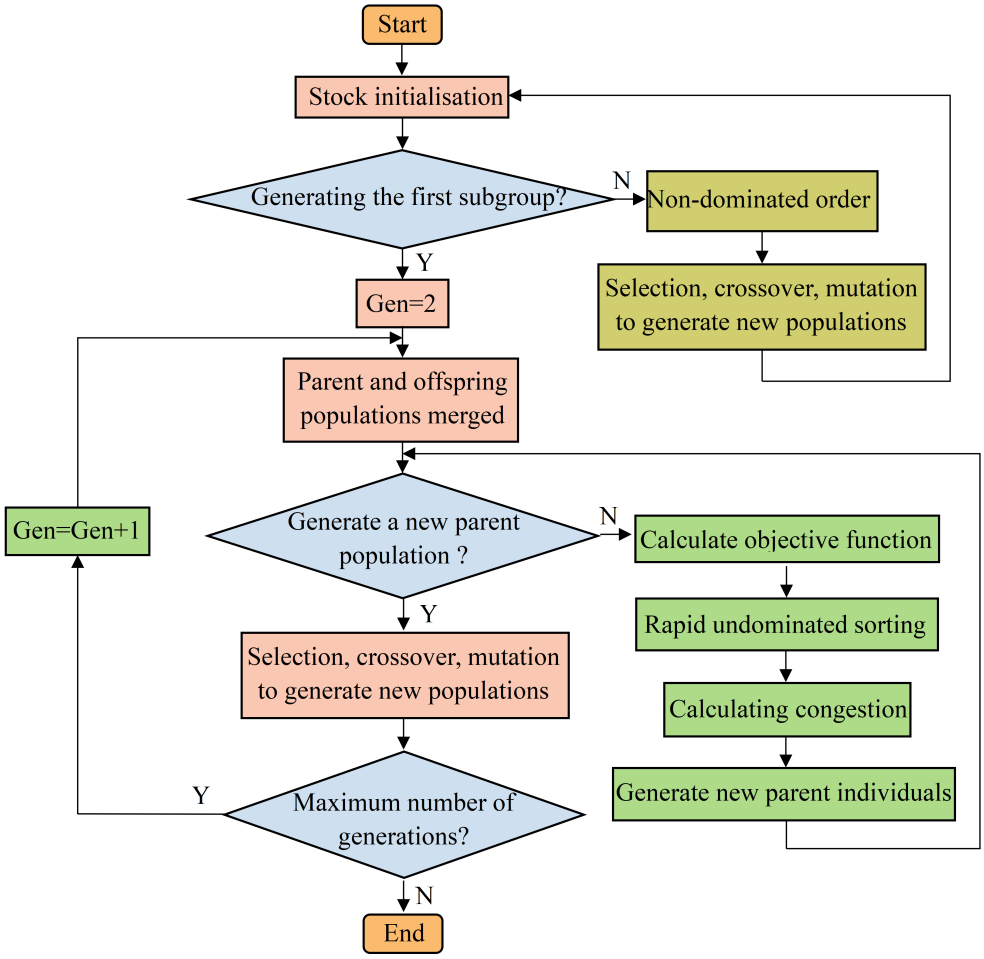

Figure 10. NSGA-II algorithm flowchart.

3.3.2. ANSYS–MATLAB Co-Simulation Method

This study utilized the ANSYS–MATLAB co-simulation technique, which combined the efficient parametric modeling and post-processing capabilities of ANSYS with the strong data processing and algorithm development functions of MATLAB [39]. ANSYS and MATLAB exchanged data through the "crood.txt" and "res.txt" files, respectively. This allowed them to monitor the calculation status in real time and determine if the calculation was complete. By synchronizing their operations, the two subsystems enhanced simulation efficiency and improved screening accuracy. The precise computational procedures are illustrated in Figure 11.

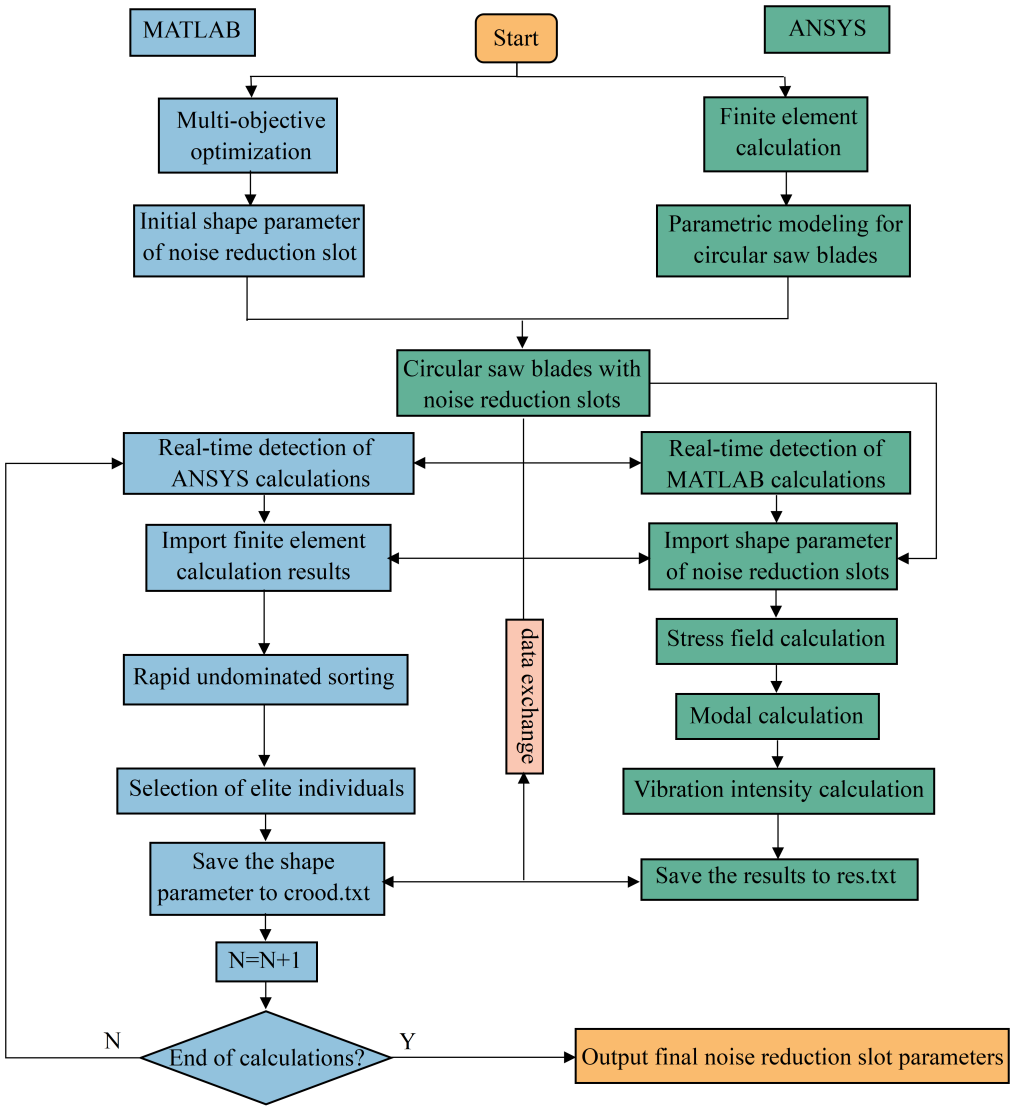

Figure 11. ANSYS–MATLAB co-simulation computational flow.

Step 1 MATLAB randomly generated a set of shape parameters within the design space as the initial population for the optimization process. Based on the radial distances and angles of the shape parameters, the corresponding Cartesian coordinates were calculated. Subsequently, the coordinate data underwent preprocessing, including data format unification, missing and duplicate value checking, and data sorting, to enhance the accuracy of curve fitting. Furthermore, the fitting curve type was defined as "poly4", and the fit function was employed to perform curve fitting on the coordinate data, yielding the fitting results. Finally, the fitted curve was discretized into

100 equally spaced coordinate points, and the coordinate information was stored in the "crood.txt" file.

Step 2 In ANSYS, the circular saw blade model (without noise-reduction slots) was first constructed. Then, a macro file containing the coordinate information of the noise-reduction slots was read to complete the parametric modeling of the circular saw blade with noise-reduction slots, as illustrated in Figure 3. Subsequently, preprocessing commands such as mesh generation and boundary condition application were executed to prepare for the subsequent analysis.

Step 3 ANSYS conducted a static analysis, prestressed modal analysis, and harmonic response analysis. The maximum deformation, maximum equivalent stress, and cumulative sum of overall vibration intensity were computed, and the data were saved in a file named "res.txt".

Step 4 MATLAB interpreted the analytical results and considered the calculated results as the fitness value of the genetic algorithm. Based on the computational procedure outlined in Figure 10, non-dominant sorting was performed to identify the most exceptional individuals.

Step 5 The shape parameter of the elite individual was considered as the fundamental parameter for optimizing the next generation. Step 1 to Step 4 were repeated until the predetermined algebraic condition was met.

4. Results and Discussion

4.1. Optimization Results and Analysis

The NSGA-II population size was set to 50, with a crossover probability of 0.80 and a mutation probability of 0.05 [40]. After 50 iterations, a total of four groups of optimal solution sets that met the criteria of the example were obtained. To simplify the categorization of various circular saw blades, those without noise reduction slots were assigned the number 0, while those with noise reduction slots were assigned the numbers 1, 2, 3, and 4 in the optimization scheme. The shape parameters are shown in Table 5, while the finite element model is depicted in Figure 12. The comparison of optimized target data is shown in Table 6.

Table 5. Optimal solution's shape parameters.

Number	Origin Radius (mm)	Endpoint Radius (mm)	Slot Width (mm)	Initial Angle	Key Point One Angle	Key Point Two Angle	Key Point Three Angle	Key Point Four Angle	Terminal Angle
1	**103.05**	**126.66**	**0.30**	**−6.71**	**−0.12**	**−8.20**	**4.72**	**−1.14**	**6.05**
2	**97.62**	**125.91**	**0.84**	**−6.89**	**−5.91**	**−7.94**	**−7.69**	**−4.82**	**8.85**
3	98.20	126.64	0.76	−1.35	−4.72	4.24	−2.84	6.46	0.37
4	101.47	126.20	0.84	3.78	−3.76	−2.16	−3.20	2.91	0.31

Table 6. Optimized target data comparison.

Number	Maximum Deformation (μm)	Maximum Equivalent Stress (MPa)	Cumulative Sum of Overall Vibration Intensity
0	10.26	23.38	766,423
1	**10.40**	**27.87**	**360,482**
2	**10.38**	**28.98**	**394,876**
3	10.37	26.80	460,954
4	10.39	26.75	578,410

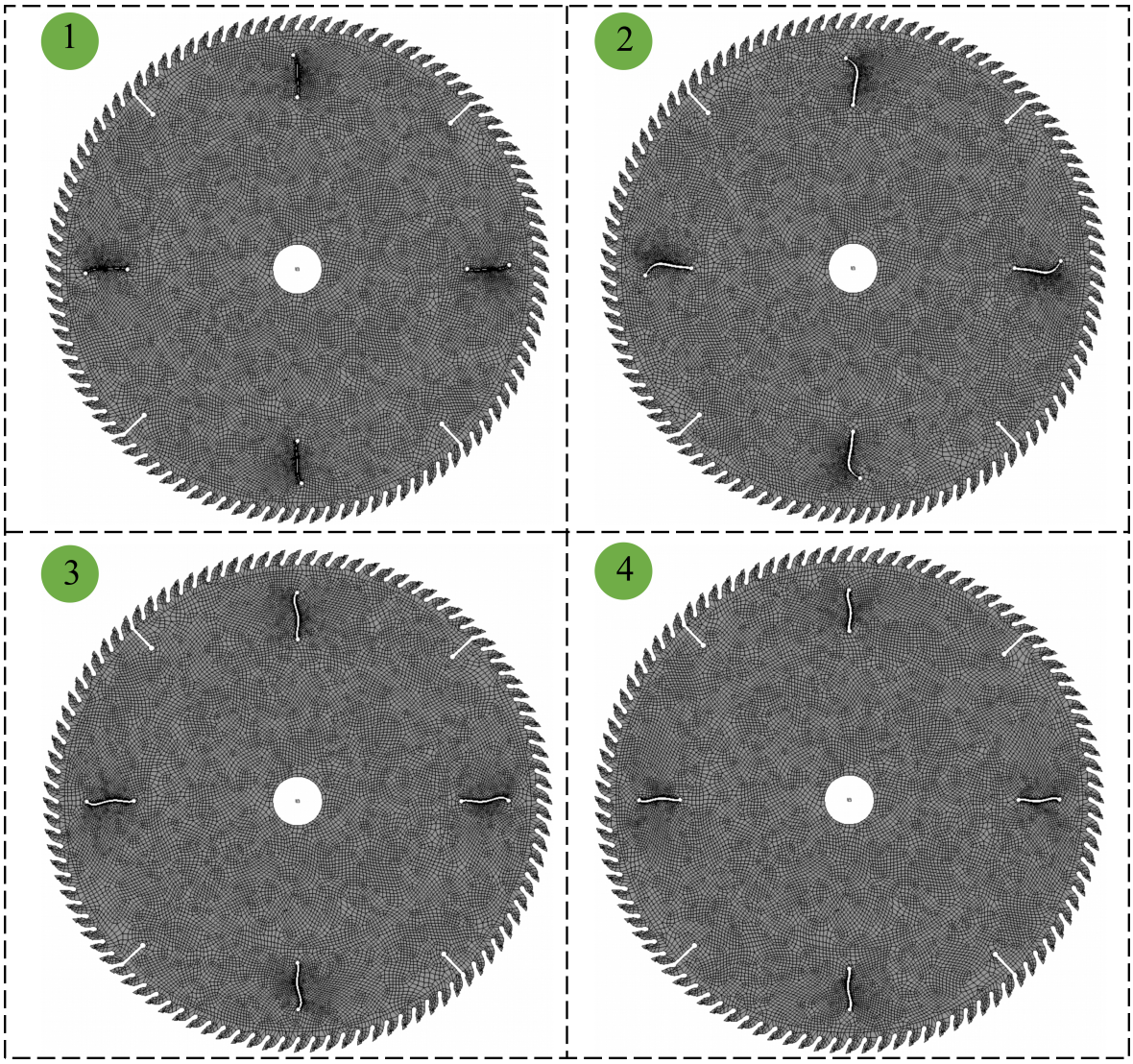

Figure 12. Optimized circular saw blade models.

Within the acquired set of Pareto front solutions, it is evident that solutions 3 and 4 had commendable performance in terms of maximum deformation and maximum equivalent stress, which were the two single-objective functions. However, their performance in relation to the other objective functions was not excellent. To ensure the overall effectiveness of the final design solution, we selected the solutions from the optimal solution set that performed well on multiple objective functions. Solutions that had single-objective optimality but lacked optimal overall performance were eliminated. As a result, solutions numbered 1 and 2 were chosen as the final optimization results.

The comparative examination of Figures 13 and 14 revealed a notable disparity in vibration response between the circular saw blade and the circular saw blade with noise reduction slots. Figure 13 illustrates the frequency response curves of the three types of circular saw blades, while Figure 14 presents a comparison of the vibration modes of the three types of circular saw blades at an excitation frequency of 1180 Hz. The optimized circular saw blade exhibited a notable decrease in the overall vibration intensity. The initial circular saw blade exhibited a pronounced and powerful vibration pattern at the excitation frequency of 1180 Hz. However, by implementing a noise reduction slot, the vibration energy at this frequency was greatly reduced, effectively preventing the occurrence of strong vibration patterns. This also validated the use of the overall vibration intensity as a reliable indicator of the circular saw blade's vibration characteristics.

Figure 15 demonstrates the difference in stress distribution between the circular saw blade with noise reduction slots and the initial circular saw blade. The results show that the initial circular saw blade had equivalent stress concentrations at the root of the saw teeth or at the inner bore, and these regions acted as free ends to release stresses [41]. However, the presence of noise reduction slots interrupted the structural continuity of the circular saw blade, and new stress concentration zones were formed at the end of the slots. Although thermal stresses were mostly concentrated at the root of the serrated section, their values were usually much smaller than the centrifugal stresses, and thus one end of the noise reduction slots became the location of the largest stress concentration.

In this scenario, the optimized two-slotted circular saw blades saw a minimal increase in maximum equivalent stress, specifically by 4.5 MPa and 5.6 MPa. The base material SKS51 has a standard tensile strength of 510 MPa. Typically, 60% of this tensile strength, which is equivalent to 306 MPa, is considered as the acceptable stress. Consequently, a stress safety factor of 10.63 was computed, which significantly exceeded the need for a safety factor (greater than 5). Therefore, the slotted circular saw blade satisfied the engineering application criteria in terms of structural strength.

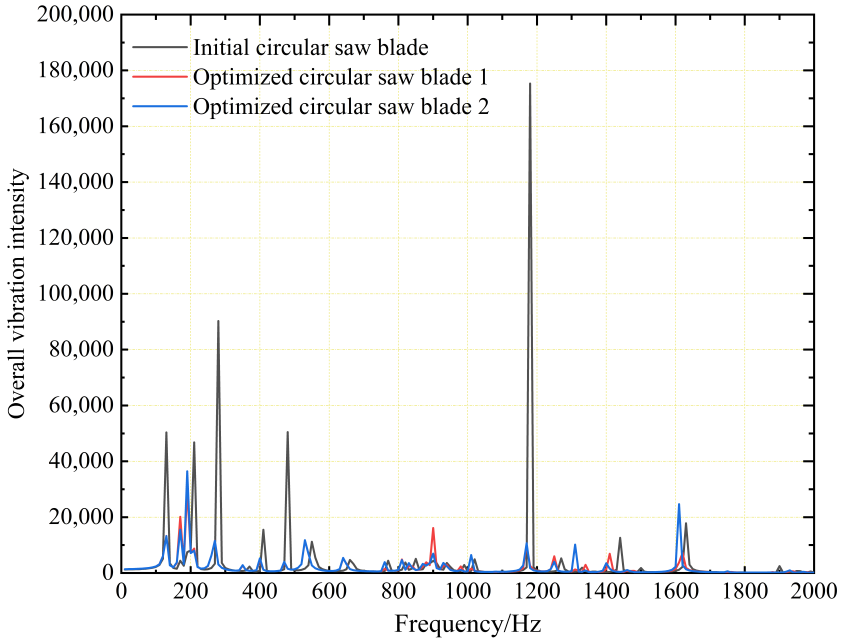

Figure 13. Comparison of overall vibration intensity spectrum.

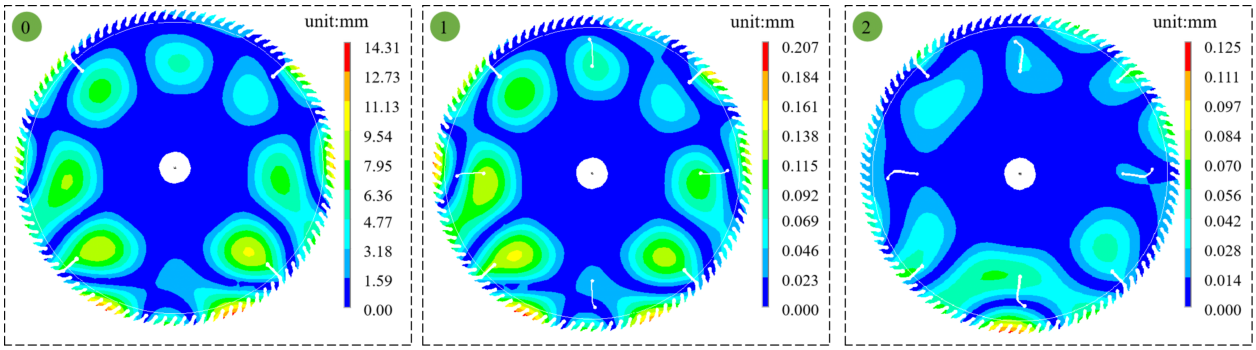

Figure 14. Vibration pattern of three circular saw blades at 1180 Hz.

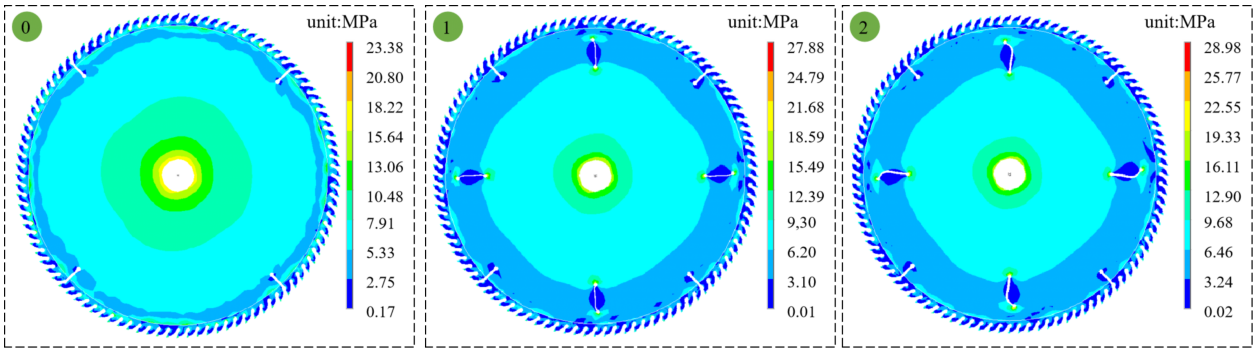

Figure 15. Stress charts for three types of circular saw blades.

4.2. Noise Test Results and Analysis

In order to evaluate the influence of the noise reduction slot on the circular saw blade's sawing noise reduction effect, based on the optimized design parameters of the noise reduction slot, the initial circular saw blade and circular saw blades 1 and 2 were successfully prepared using the laser grooving technology, as shown in Figure 16. The size of the particleboard specimens used in the experiments was 100 mm in length, 50 mm in width, and 2 mm in height, and the relevant mechanical parameters are shown in Table 4.

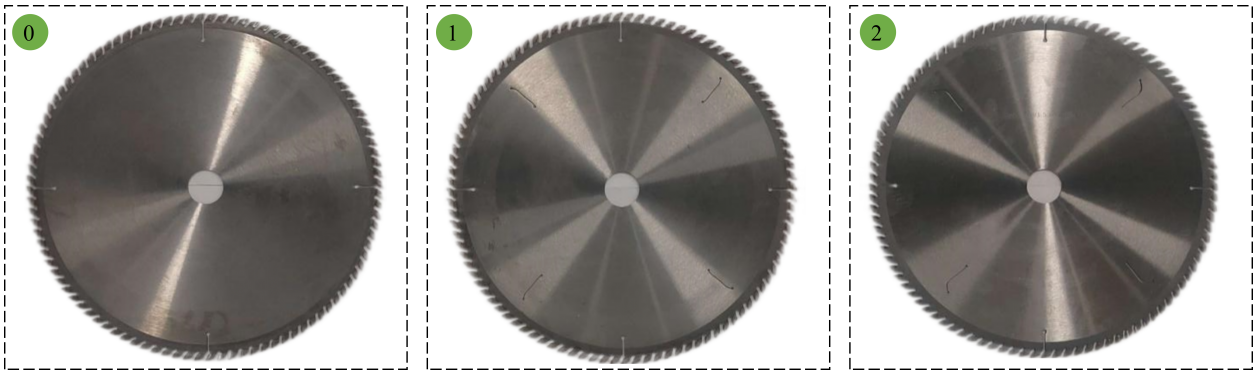

Figure 16. Ultra-thin circular saw blades.

A precision board cutting saw (China Shenyang Baoshan Woodworking Equipment Factory MJ-90) was used to cut the boards for the project. A sound level meter (China Hangzhou Aihua Instrument Co., Ltd., Hangzhou, China, AWA-6292) was used to record the noise from the sawing. It was put 1 m away from the sawing and lined up straight with the main axle box axis of the precision board cutting saw [42]. The sound level meter can perform both time weighting (F, S, I) and frequency weighting (A, C, Z). It can also conduct total value integration and one-third-octave spectrum analysis. It can measure between 20 dB and 143 dB and handle sampling frequencies between 20 Hz and 20 kHz. Figure 17 shows the test site and schematic diagram.

During the noise measurement evaluation, the sound pressure levels of three circular saw blades were recorded in both idle and sawing circumstances. The measurements were taken at a 1 s interval. The audio was then separated into frequency bands using the one-third-octave method. This allowed for the analysis of the spectrum features of the circular saw blades.

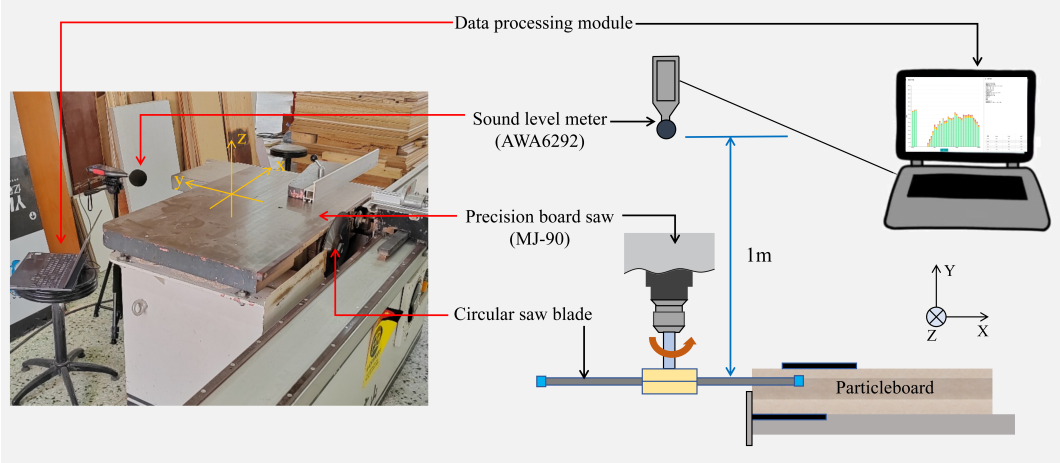

Figure 17. Noise test site and schematic diagram.

1. The optimized circular saw blade, as depicted in Figure 18, demonstrated reduced sound radiation ability during the stable sawing phase. On average, there was a decrease in sound pressure level of approximately 2.4 dB to 3.0 dB. This outcome suggested that the design solution made some improvement in the overall noise level. During the idle stage of the circular saw blade, known as the saw-in and saw-out stages, there was minimal difference in the sound radiation capacity between the circular saw blade with noise reduction slots and the original circular saw blade. This suggested that the modifications made to the circular saw blade body had little impact on the equivalent sound pressure level during its idle stage, which aligns with the findings of the study conducted by Ján Svoren et al. [43]. Furthermore, the research conducted by Tian et al. [44] highlighted that decreasing the diameter of the saw blade, suitably increasing the number of teeth on the saw blade, and reducing the thickness of the saw blade were excellent methods for minimizing the idle noise produced by the saw blade.
2. According to Figure 19, the noise radiation level of the optimized circular saw blade was lower than the initial design in most of the frequency bands. The reduction was particularly significant in the frequency range of 500 Hz to 1600 Hz. This reduction in noise was consistent with the decrease in overall vibration intensity of the circular saw blade after optimization, as shown in Figure 13.
   It is important to mention that while the noise levels of the optimized circular saw blades were typically lower than those of the original saw blades, the sound pressure level values of saw blade 2 in the frequency range of 1600 Hz–2000 Hz were slightly higher. This behavior could be attributed to the occurrence of excitation during the sawing process that aligned with a specific inherent frequency of the optimized circular saw blade 2. As a result, there was a notable increase in the emission of noise within this frequency range. Furthermore, minor variations in the design and composition of the circular saw blade and plate material could also have an impact on the noise level, making it difficult to completely avoid in the design process.

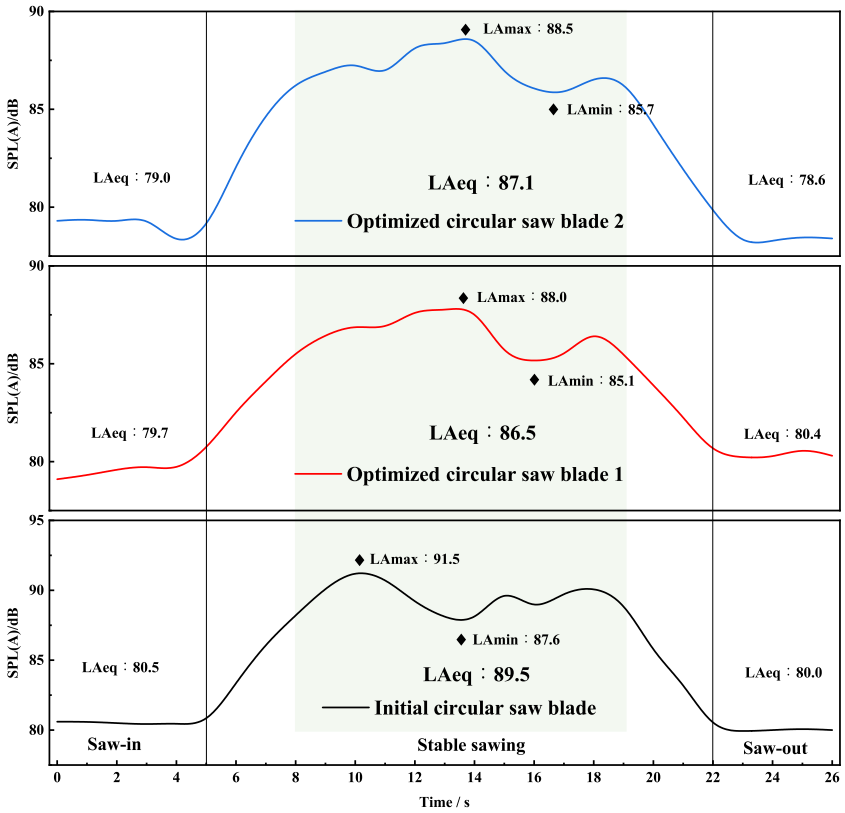

Figure 18. Equivalent sound pressure level curves for three types of circular saw blades.

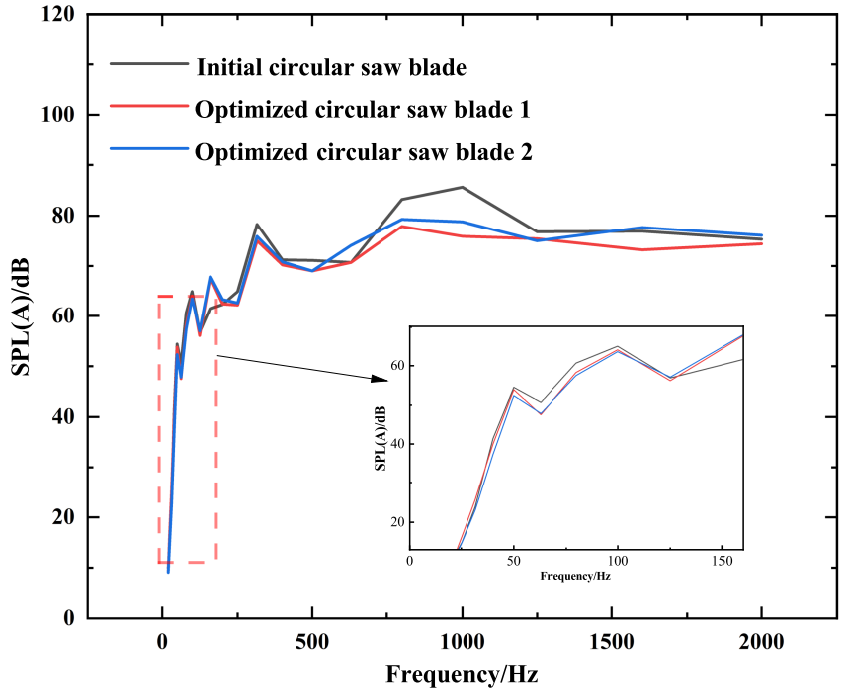

Figure 19. Comparison of 1/3-octave spectra of saw cut noise.

5. Conclusions

This study presented a mathematical model to reduce vibration and noise in circular saw blades. It utilized the ANSYS–MATLAB joint simulation platform to apply multi-objective optimization technology, offering an innovative solution for designing noise reduction slot in ultra-thin circular saw blades. The main findings were as follows.

1. A mathematical model for reducing vibration and noise in circular saw blades was derived. It established a mathematical relationship between the sound power emitted and the overall vibration intensity of the circular saw blade system. Furthermore, it established a direct mapping between the shape parameters of the noise reduction slot in the circular saw blade and the sawing deformation, equivalent stress, and overall vibration intensity. This led to the construction of a multi-objective optimization model for the noise reduction slot. This approach enhanced both the computational efficiency and the effectiveness of mathematical tools for controlling vibration noise in circular saw blade design and engineering applications.
2. The suggested approach utilized a thermal–mechanical coupling analysis, prestress modal analysis, and harmonic response analysis to accurately determine the overall vibration intensity of circular saw blades. The method considered the impact of the stress state on the vibration characteristics of rotary circular saw blades. It could calculate the overall vibration intensity of various circular saw blades cutting different materials at any frequency range. This calculation can aid in the design and development of vibration and noise reduction for circular saw blades and other rotary cutters.
3. A simulation platform was developed using ANSYS and MATLAB to determine the best shape parameters of noise reduction slots for ultra-thin circular saw blades used in cutting particleboards. NSGA-II was employed for this purpose. The multi-objective optimization method simultaneously achieved the design of reducing vibration and noise in the ultra-thin circular saw blade, while also ensuring that the circular saw blade maintained the requisite rigidity and strength requirements after grooving. The utilization of the joint simulation technique guaranteed precise data transmission, enhanced design efficiency, and showcased a broad scope of versatility and practicality. This served as a valuable reference for designing slots for various other types of circular saw blades.
4. The preparation of slotted circular saw blades was carried out according to the optimization results. The experimental results demonstrated a reduction in sawing noise by 2.4 dB to 3.0 dB. Additionally, the noise levels of the optimized circular saw blades were generally lower than those of the initial saw blades across most of the design frequency bands. This finding aligned well with the overall reduction in vibration intensity, confirming the validity and practicality of the design scheme.

To further enhance the usefulness and applicability of the methodology, future research and development may start from the following.

1. Multi-scale multi-physical field coupling problem of sawing system: There are certain simplifications in the currently adopted finite element model, such as ignoring the chip formation process, contact nonlinearity problem, etc. The establishment of a high precision multi-scale simulation model of the wood sawing system, from the microscopic material behavior to the macroscopic cutting process for a comprehensive description, to provide a more reliable theoretical basis for the optimal design. In addition, the comprehensive use of mechanics, acoustics, fluids, and other related disciplines to reveal the vibration and noise generation mechanism of circular saw blades under the conditions of multi-physical field coupling is still the focus of the current research issues.
2. Broader frequency analysis: This study focused on a specific frequency range, and future research could extend the analysis to a broader frequency range, especially frequencies outside the current range. This would ensure that the circular saw blade is optimized for a wider range of operating conditions.
3. Machine learning method: This optimization calculation method allows saw blade design for specific materials or cutting requirements but requires complex code adjustments each time. The application of machine learning technology would reduce the computational time and resources required for simulation studies by accumulating a

large quantity of simulation and experimental data under cutting conditions and predicting performance results based on historical data to refine the optimization process.

Author Contributions: Conceptualization, N.J. and L.G.; methodology, L.G.; software, L.G.; validation, N.J. and L.G.; formal analysis, R.W.; investigation, N.J.; resources, R.W.; data curation, L.G.; writing original draft preparation, L.G.; writing—review and editing, N.J.; visualization, L.G.; supervision, J.L.; project administration, J.L.; funding acquisition, N.J. All authors have read and agreed to the published version of the manuscript.

Funding: This work was supported by Central Guidance on Local Technology Development Special Fund: Application and Industrialization of Pure Grade Electrical Laminated Wood Preparation Technology [Grant No. ZY23CG18].

Data Availability Statement: The raw data supporting the conclusions of this article will be made available by the authors on request.

Conflicts of Interest: The authors declare no conflicts of interest.

References

1. Cho, H.S. On the aerodynamic noise source in circular saws. *J. Acoust. Soc. Am.* **1979**, *65*, 662–671. [CrossRef]
2. Bobeczko, M.S.; Henry, B.B. Noise Reduction Achieved with Slotted Blades. *Light Met. Age* **1976**, *33*, 24–31.
3. Singh, R. Case History. The effect of radial slots on the noise of idling circular saws. *Noise Control Eng. J.* **1988**, *31*, 167–172. [CrossRef]
4. Yusif, S.; Soar, J. Effect of compensation slots, cooper corks in the body of a circular saw blade and unbalanced pitch of several teeth on noise level of circular saws in cutting process. In Proceedings of the International Scientific Conference Woodworking Technique, Zaleina, Croatia, 2–5 September 2007.
5. Svoreň, J.; Javorek, Ľ.; Murín, L. Effect of the Shape of Compensating Slots in the Body of A Circular Saw Blade on Noise Level in the Cutting Process. *Pro Ligno* **2010**, *6*, 5–12.
6. Merhar, M.; Bučar, D.G. The Influence of Radial Slots on Dynamic Stability of Thermally Stressed Circular Saw Blade. *Drv. Ind.* **2017**, *68*, 341–349. [CrossRef]
7. Li, Y. Influence of Radial Slots on the Vibration Characteristics of Circular Saw Blade. *Appl. Mech. Mater.* **2012**, *226–228*, 232–236.
8. Chen, K.N.; Chang, C.; Huang, J.C. Optimum design of diamond saw blades based on experimentally verified finite element models. *Comput.-Aided Des. Appl.* **2012**, *9*, 571–583. [CrossRef]
9. Gau, W.H.; Chen, K.N.; Hwang, Y.L. Model Updating and Structural Optimization of Circular Saw Blades with Internal Slots. *Adv. Mech. Eng.* **2014**, *2014*, 546496.
10. Wu, T.; Wang, D.; Zhao, M. Optimization of diamond circular saw blade by vibration noise analysis. *IOP Conf. Ser. Mater. Sci. Eng.* **2021**, *1138*, 012045.
11. Tian, Y.; Xu, G.; Zhang, X.; Duan, G. Research on structural optimization of diamond circular saw blade under multi-constraints conditions. *J. Vib. Shock* **2020**, *39*, 8.
12. Verma, S.; Pant, M.; Snasel, V. A Comprehensive Review on NSGA-II for Multi-Objective Combinatorial Optimization Problems. *IEEE Access* **2021**, *9*, 57757–57791. [CrossRef]
13. Xiao, W.; Cheng, A.; Li, S.; Jiang, X.; Ruan, X.; He, G. A multi-objective optimization strategy of steam power system to achieve standard emission and optimal economic by NSGA-II. *Energy* **2021**, *232*, 120953. [CrossRef]
14. Xu, J.; Zhong, G.; Yang, S. Improved NSGA-II algorithm and its application in optimization of machining parameters. *Comput. Eng. Appl.* **2017**, *53*, 227–234.
15. Ahmadi, A.A.; Arabbeiki, M.; Ali, H.M.; Goodarzi, M.; Safaei, M.R. Configuration and optimization of a minichannel using water–alumina nanofluid by non-dominated sorting genetic algorithm and response surface method. *Nanomaterials* **2020**, *10*, 901. [CrossRef]
16. Tan, W.; Yuan, X.; Yang, Y.; Wu, L. Multi-objective casting production scheduling problem by a neighborhood structure enhanced discrete NSGA-II: An application from real-world workshop. *Soft Comput.* **2022**, *26*, 8911–8928. [CrossRef]
17. Nguyen, V.K.; Pham, H.T.; Pham, H.H.; Dang, Q.K. Optimization design of a compliant linear guide for high-precision feed drive mechanisms. *Mech. Mach. Theory* **2021**, *165*, 104442. [CrossRef]
18. Tian, Y.; Xu, G.; Zhao, H.; Duan, G. Dynamic topology optimization design of low noise diamond circular saw blades. *J. Vib. Shock* **2019**, *38*, 7.
19. Mote C., Jr. Stability of circular plates subjected to moving loads. *J. Frankl. Inst.* **1970**, *290*, 329–344. [CrossRef]
20. Song, X.; Zhai, J.; Chen, Y.; Han, Q. Traveling wave analysis of rotating cross-ply laminated cylindrical shells with arbitrary boundaries conditions via Rayleigh–Ritz method. *Compos. Struct.* **2015**, *133*, 1101–1115. [CrossRef]
21. Yao, T.; Duan, G.; Cai, J. Review of vibration characteristics and noise reduction technique of circular saws. *J. Vib. Shock* **2008**, *27*, 162–166.
22. Svoreň, J.; Naščák, L.; Barcík, Š.; Koleda, P.; Stehlík, Š. Influence of circular saw blade design on reducing energy consumption of a circular saw in the cutting process. *Appl. Sci.* **2022**, *12*, 1276. [CrossRef]

23. Wang, X.L.; Yin, Z.J.; Li, Y.L. The stress analysis of different circular saw structures during cutting. *Adv. Mater. Res.* **2011**, *228*, 471–476. [CrossRef]
24. Lin, L.; Wen, Q.; Wang, C. Structural topology optimization of circular saw blade. *J. Mach. Des.* **2018**, *35*, 24–28.
25. Yu, M.; Wang, B.; Zhang, L.; Li, B.; Zhang, Q. Comparison of tensioning effect between roll and multi-spot pressure tensioning process of circular sawblade. *Wood Mater. Sci. Eng.* **2023**, *18*, 1827–1840. [CrossRef]
26. Gamage, N.; Setunge, S. Modelling of vertical density profile of particleboard, manufactured from hardwood sawmill residue. *Wood Mater. Sci. Eng.* **2015**, *10*, 157–167. [CrossRef]
27. *GB/T 17657-2022*; Physical and Chemical Properties Test Methods for Wood-Based Panels and Surface Decorated Wood-Based Panels. State Administration for Market Regulation; Standardization Administration of the P.R.C: Beijing, China, 2022.
28. Feng, Q.; Zhang, M.; Gong, J. Experimental and numerical study on pyrolysis and autoignition of OSB exposed to radiant heat fluxes. *China Saf. Sci. J.* **2022**, *32*, 137–143. [CrossRef]
29. Bejo, L.; Lang, E.M.; Fodor, T. Friction coefficients of wood-based structural composites. *For. Prod. J.* **2000**, *50*, 39.
30. Chen, Q.; Li, D. A computational study of frictional heating and energy conversion during sliding processes. *Wear* **2005**, *259*, 1382–1391. [CrossRef]
31. Ding, Y.; Ma, Y.; Liu, T.; Zhang, J.; Yang, C. Experimental Study on the Dynamic Stability of Circular Saw Blades during the Processing of Bamboo-Based Fiber Composite Panels. *Forests* **2023**, *14*, 1855. [CrossRef]
32. Cobb, E.; Saunders, O. Heat transfer from a rotating disk. *Proc. R. Soc. Lond. Ser. A Math. Phys. Sci.* **1956**, *236*, 343–351.
33. Czajkowski, Ł.; Olek, W.; Weres, J.; Guzenda, R. Thermal properties of wood-based panels: Specific heat determination. *Wood Sci. Technol.* **2016**, *50*, 537–545. [CrossRef]
34. Yu, M.; Wang, B.; Ji, P.; Li, B.; Zhang, L.; Zhang, Q. Study on the dynamic stability of circular saw blade during medium density fiberboard sawing process with thermo-mechanical coupling. *Comput. Electron. Agric.* **2023**, *211*, 108042. [CrossRef]
35. Li, S.; Wang, C.; Zheng, L.; Wang, Y.; Xu, X.; Ding, F. Dynamic stability of cemented carbide circular saw blades for woodcutting. *J. Mater. Process. Technol.* **2016**, *238*, 108–123. [CrossRef]
36. Rieß, S.; Kaal, W.; Herold, S. Vibration reduction on circular saw blades with vibroacoustic metamaterials. *Bull. Pol. Acad. Sci. Tech. Sci.* **2023**, *71*, 1–2 . [CrossRef]
37. Wu, B.; Yang, S.; Li, Z.; Zhong, H.; Chen, X. Computation of frequency responses and their sensitivities for undamped systems. *Eng. Struct.* **2019**, *182*, 416–426. [CrossRef]
38. Deb, K.; Pratap, A.; Agarwal, S.; Meyarivan, T. A fast and elitist multiobjective genetic algorithm: NSGA-II. *IEEE Trans. Evol. Comput.* **2002**, *6*, 182–197. [CrossRef]
39. Gong, W.; Zhu, Z.; Wang, K.; Yang, W.; Bai, Y.; Ren, J. A real-time co-simulation solution for train–track–bridge interaction. *J. Vib. Control* **2021**, *27*, 1606–1616. [CrossRef]
40. Konak, A.; Coit, D.W.; Smith, A.E. Multi-objective optimization using genetic algorithms: A tutorial. *Reliab. Eng. Syst. Saf.* **2006**, *91*, 992–1007. [CrossRef]
41. Yıldırım, V. A parametric study on the centrifugal force-induced stress and displacements in power-law graded hyperbolic discs. *Lat. Am. J. Solids Struct.* **2018**, *15*, e34. [CrossRef]
42. Krilek, J.; Kováč, J.; Barcík, Š.; Svoreň, J.; Štefánek, M.; Kuvik, T. The influence of chosen factors of a circular saw blade on the noise level in the process of cross cutting wood. *Wood Res.* **2016**, *61*, 475–486.
43. Svoreň, J.; Naščák, L.; Koleda, P.; Barcík, Š.; Němec, M. The circular saw blade body modification by elastic material layer effecting circular saws sound pressure level when idling and cutting. *Appl. Acoust.* **2021**, *179*, 108028. [CrossRef]
44. Tian, Y.; Duan, G.; Xia, X.; Zhang, E. Calculations and Analyses on Aerodynamic Noise Characteristics of Rotating Saw Blades. *China Mech. Eng.* **2017**, *28*, 272–278.